

Forming Real-World Human-Robot Cooperation for Tasks with General Goal

Lingfeng Tao¹, Michael Bowman¹, Jiucui Zhang² and Xiaoli Zhang¹, *Member, IEEE*

Abstract—In human-robot cooperation, the robot cooperates with humans to accomplish the task together. Existing approaches assume the human has a specific goal during the cooperation, and the robot infers and acts toward it. However, in real-world environments, a human usually only has a general goal (e.g., general direction or area in motion planning) at the beginning of the cooperation, which needs to be clarified to a specific goal (i.e., an exact position) during cooperation. The specification process is interactive and dynamic, which depends on the environment and the partner’s behavior. The robot that does not consider the goal specification process may cause frustration to the human partner, elongate the time to come to an agreement, and compromise team performance. This work presents the Evolutionary Value Learning approach to model the dynamics of the goal specification process with State-based Multivariate Bayesian Inference and goal specificity-related features. This model enables the robot to enhance the process of the human’s goal specification actively and find a cooperative policy in a Deep Reinforcement Learning manner. Our method outperforms existing methods with faster goal specification processes and better team performance in a dynamic ball balancing task with real human subjects.

I. INTRODUCTION

Human-robot cooperation (HRC) is a promising topic in many applications, such as manufacturing [1], complex surgery [2] and autonomous driving [3]. For all HRC, the robot should adapt to the human to maintain healthy cooperation and help the human to achieve their goal [4]. Existing approaches in HRC assume the human has a specific goal at the beginning of the cooperation [5], where there is one or multiple targets pre-known to the robot (e.g., exact locations or objects). The human may act toward one of these targets or change from one target to another. In these scenarios, the human always applies actions toward a specific target. However, this assumption may not be accurate in real-world applications. A common experience in real-life cooperation is that the team may hover around the expected area to find the best location/target/solution that satisfies all team members. We identify that *in realistic cooperation, the human may not have a specific goal at the beginning of the task but instead start with a general goal (e.g., a higher-level direction or area). The cooperation is a process where the goal starts as a general idea and becomes more specific as the task continues (e.g., a target direction to a target location).* Furthermore, the goal specification and the corresponding

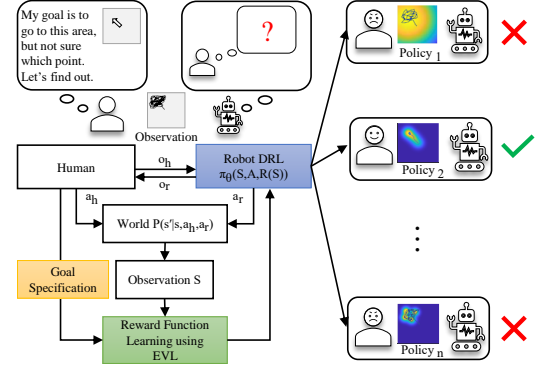


Fig. 1. In realistic cooperation, the human may not have specific targets at the beginning of one task, but rather start with a higher-level goal (i.e., a general direction or area). In this work, the robot learns a cooperative policy in a Deep Reinforcement Learning (DRL) manner (blue block). The human specifies the goal with the help of the robot (yellow block). Then the observation and information of the goal specification process are used to learn a reward function using the proposed Evolutionary Value Learning algorithm. A good policy, like Policy 2, helps the human to clarify the goal and achieve healthy cooperation. Bad policies, like Policy 1, are too broad thus may frustrate the user. Policy n is too specific on data that it misses the human’s actual goal.

cooperation formation are interactive and dynamic, whose final equilibrium or agreement depends on the task and partner behaviors. Different cooperation processes can end up with different final equilibrium/agreements and different performances. This is due to human actions usually reactively choosing to specify the goal. *Thus, the robot needs to assist the human during the goal specification process to achieve better HRC when the human only has a general goal.*

In traditional HRC methods, the robot does not usually take the goal specification process into account because of the specific goal assumption. The goal inference is simplified to a classification problem where the robot identifies a single discretized goal such as an object of interest to grasp or a specific way/routine for task execution. Then, the robot only needs to find which target is the human’s goal and generate actions to assist the human. In contrast, a general goal is abstract and unclear. The human usually has no specific target for the robot to predict (classify), making it more difficult to form the cooperation.

The probability-based goal inference approaches, such as Bayesian inference [6], iteratively infer a human’s goal based on observation. These studies still assume the human has a specific goal; it is the robot who is not certain of the human’s goal. So, it infers the human’s goal with a form of probability fusion. However, when the human has no specific goal, the inference usually has low confidence and high variance because the human’s reactive behaviors when specifying the

¹L. Tao, M. Bowman, and X. Zhang are with Colorado School of Mines, Intelligent Robotics and Systems Lab, 1500 Illinois St, Golden, CO 80401 USA (e-mail: tao@mines.edu, mibowman@mines.edu, xlzhang@mines.edu).

²J. Zhang is with the GAC R&D Center Silicon Valley, Sunnyvale, CA 94085 USA (e-mail: zhangjiucui@gmail.com).

goal may mislead the robot in the wrong direction. It also lacks the ability to memorize past human behaviors. It is difficult for the inference model to follow a potential target the human previously experienced and wants to recall from the distant past.

The learning-based approaches like Inverse Reinforcement Learning (IRL) [7] learn the human goal from the demonstration (i.e., trajectory). However, when considering a general goal, the human may end up with different task/cooperation equilibrium in different trials during the goal specification process, which are inconsistent for learning. In such conditions, current HRC methods are limited when modeling or inferring the general goal, resulting in the human's adaption or correction to the robot's behavior rather than vice versa.

This work presents an Evolutionary Value Learning (EVL) approach to first build an abstract goal inference model from the observation with a State-based Multivariate Bayesian Inference (SMBI) method. SMBI model continuously covers the environment's state space, which does not require discretized representation of specific targets. Meanwhile, the robot experience is then used to extract the goal specificity-related features describing the human's historical goal specification process. Finally, EVL uses the probability distributions of these features to iteratively shape the SMBI model to build an adaptive model of the human's general goal. The global perspective of the evolutionary value model can naturally turn into a reward function for the robot to solve the HRC under a Reinforcement Learning (RL) manner. The contribution of this work is summarized as follow:

- 1) **Development of an Evolutionary Value Learning (EVL) approach** that includes:
 - a) **A State-based Multivariate Bayesian Inference (SMBI)** to model the dynamics of the goal specification process online with a global perspective.
 - b) **An Evolutionary Value updating method** to actively generate the evolutionary reward function with the SMBI model and offline feature extraction to enhance the process of goal specification and cooperation formation.
- 2) **Validation of the EVL approach** with human subjects in a dynamic task using a straightforward visualization of the HRC and goal specification process.

II. RELATED WORK

Conventional human goal prediction methods build inference models on three types of objectives. The first type is the target-based objective, where the robot infers the human's target and helps the human reach the target, such as an object grasping task [8]. The second type is routing-based objective, where the robot infers what routing the human is following and helps to finish the rest of the steps, such as a cooperative cooking task [9]. The third one is the action-based objective, where the robot predicts which action the human will execute, such as a table-carrying task [10]. The robot needs to predict the human's action plan, both rotational and translational components. Overall, the above

approaches are built under the assumption that the human has a specific goal when deciding the object of interest, executing the routing, or generating an action plan, which may not work appropriately if the human only has a general goal.

Literature has used Bayesian Inference (BI) methods to build target-based human goal predictive models from human behavior observation. BI iteratively updates the posterior probability of the human's goal according to the observed information. For example, a multi-class BI model can be used to predict the human's goal of grasping [11]. BI was also used to learn a transition function to describe how humans select a target [12]. This approach infers the goal with partially observed human behavior, yet still assumes that the human has a specific goal among several known targets. A potential problem of current Bayesian approaches is that the posterior is updated with the online observations. For instance, let us consider when the human goal is not specified. During the early specification process, real-time human behavior and states may not sufficiently convey the goal's information which leads to the robot making errant actions. Furthermore, when the human wants to recall a visited target in the distant past, BI methods cannot quickly follow the human due to its inability to memorize sparse information [13].

Learning-based methods are popular to enable robots to understand the human goal. Literature has used IRL in HRC to build empirical reward functions based on human demonstrations [14]. The empirical reward function is then used in an RL setting to guide the policy learning process. Recent approaches such as Cooperative IRL [15] (also known as value alignment), shows that humans can actively teach the robot to cooperate in HRC. However, such learn-from-demonstration approaches require humans to act optimally with dependable demonstrations (i.e., a specific goal) [16]. Although some methods like [17] allow the human to have different ways to achieve the goal (i.e., different routes), it is still assumed that the goal is specific because the final states are the same. Thus, the IRL method is unlikely feasible when the human has a general goal.

Human-in-the-loop algorithms attempt to learn human value while robots and humans interact with the environment [18], such as a cooperative assembly task [19]. Literature has used a reinforcement function [20] to model the relationship between the state-action pairs and the human's values to be learned by the RL agent. Human-in-the-loop algorithms assume the human can give optimal actions, and the human's role is to guide the robot to learn the policy. This work focuses on enabling the robot to help the human specify the goal together rather than the other way around.

III. EVOLUTIONARY VALUE LEARNING

A. Model Structure

We model the HRC as an RL problem that follows the Markov Decision Process (MDP) [21]. The MDP is defined as a tuple $\{S, A, R, \gamma\}$, where $\{a_h, a_r\} \in A$ is the set of actions of the human and the robot, R is the reward function that gives the reward after a transition from state s_t to state s_{t+1} .

γ is a discount factor to scale down the future rewards so that the cumulative rewards remain bounded. A policy $\pi(s, \theta)$ specifies an action for state s with the network parameters of θ , which are the bias and weights in a deep neural network. To find θ , Proximal Policy Optimization (PPO) algorithm [22] is adopted. It is a model-free, online, on-policy reinforcement learning algorithm. The PPO algorithm is a type of stochastic policy gradient descent approach that alternates between sampling data through environment interaction and optimizing a clipping surrogate objective function. Compared to other Deep Reinforcement Learning (DRL) methods, PPO balances ease of implementation, sample complexity, and ease of tuning. The following sections introduce SMBI (II.B) and EVL (II.C) to construct and update the reward function based on the human goal specification process.

B. State-based Multivariate Bayesian Inference (SMBI)

When a human has a general goal, prior knowledge is not available for the robot to generate an initial policy. The robot must learn to cooperate during the task. Thus, a method that can model humans in real-time is needed. Multivariate Bayesian Inference (MBI) has been recently used to model the dynamic of human behaviors in robotics. In [23], MBI was first used to model human preference with online observation. Then it was adopted in [24] to optimize an exoskeleton based on the user feedback. This section introduces SMBI, which builds a multivariate inference model of the human goal based on the observed human's exploration in the state space. An observation trajectory is denoted as $T = \{s_1, \dots, s_t, \dots, s_\Gamma\}$, where Γ is the length of the trajectory. $s_t = [d_1, \dots, d_i, \dots, d_n]$ is the state vector at time t , d_i is the state component, n is the length of the state vector. We assume there exists a latent, underlying goal $g(d_i)$ for the human (but not yet specified) for each state component d_i . So the unified goal can be written as a vector $F = [g(d_1), \dots, g(d_i), \dots, g(d_n)]^{Tr}$, Tr means transpose. Given the state s_t , we want to find the posterior probability of F :

$$P(F|s_t) \propto P(s_t|F)P(F) \quad (1)$$

we define the multivariate Gaussian prior over F :

$$P(F) = \frac{1}{\sqrt{(2\pi)^n |\Sigma|}} \exp\left(-\frac{1}{2} F^T \Sigma^{-1} F\right) \quad (2)$$

where $\Sigma \in R^{n \times n}$ is the covariance matrix, the xy th element of Σ is a Gaussian kernel K_G :

$$K_G(d_x, d_y) = \exp\left[-\frac{\Gamma}{2} \sum_{c=1}^n (d_x^c - d_y^c)^2\right] \quad (3)$$

The likelihood is the joint probability of observing the state s_t given the latent function values, which is calculated as:

$$P(s_t|F) = \prod_{i=1}^n P[d_i|g(d_i)]|t \quad (4)$$

$|t$ means at time step t . From the Bayes' theorem, the posterior $P(F|s_t)$ is:

$$P(F|s_t) = \frac{P(F)}{P(s_t)} \prod_{i=1}^n P[d_i|g(d_i)]|t \quad (5)$$

where the prior $P(F)$ is defined in (2), the likelihood function is defined in (4), the normalization factor $P(s_t) =$

Algorithm 1 Evolutionary Value Learning (EVL)

Input: Initial agent policy $\pi(\theta_0)$, initial goal prior $P(F)$

Output: Evolutionary value function V_Γ , policy π_Γ

```

1: for episode = 1, 2, ... do
2:   Obtain initial state  $s_1$ 
3:   for  $t = 1, 2, \dots, \Gamma$  do
4:     Select action  $a_t$  with policy  $\pi(s_t, \theta_{t-1})$ 
5:     Return trajectory  $[s_1, a_1, s_2, a_2, \dots, s_\Gamma, a_\Gamma]$ 
6:   end for
7:   Update posterior  $P(F|s_t)$  with (1)-(5)
8:   Update  $H_m \forall m = 1, 2, 3, 4$  with (6)-(9)
9:   Update evolutionary value function  $V_t$  with (10)
10:  Update agent policy  $\pi(s_t, \theta_t)$ 
11:  if human stop = true then
12:    Break
13:  end if
14: end for
```

$\int P(s_t|F)P(F)dg$. The posterior $P(F|s_t)$ can be estimated with the Laplace approximation method [25]. The learned inference model fully covers the environment's state space. Thus, the learned probability distribution of goal is suitable to act as the reward function for the RL training [26].

C. Evolutionary Value Learning (EVL)

Pure Bayesian methods are highly dependent on the online sample, which may not be ideal for a stable learning process, as explained in section I.B. This section introduces the EVL method, which builds an evolutionary reward function R with the posterior of the human goal $P(F|s_t)$. It is built from the SMBI model and the probabilistic human guidance features $\{H_1, \dots, H_m, \dots, H_M\}$, where M is the number of features. Each feature is a multivariate distribution over the state component d_i , which has the same dimensions as the SMBI model. In this work, we define the following features:

1) Spectral entropy [27], which can measure human behavior's spectral power distribution or information density. The distribution of the spectral entropy is defined as:

$$H_1(d_i)_t = -\sum_{i=1}^{\Gamma} d_i \log_2 P(d_i)|t \quad (6)$$

where $P(d_i) = \frac{|X(d_i)|^2}{\sum |X(d_i)|^2}$ is the probability distribution, $X(d_i)$ is the discrete Fourier transform of d_i , and t is the time step. This feature aims to encourage the robot to explore the high entropy state (i.e., high information density).

2) The frequency a state is visited gives the first-order information on how the human explores [28]. For example, the human may revisit the states that give higher reward. The robot should also visit states that are explored most of the time. The probability distribution of the state component d_i is defined to follow a kernel probability density function:

$$H_2(d_i) = \frac{1}{\Gamma} \sum_{t=1}^{\Gamma} K_U(d_i)|t \quad (7)$$

where K_U is a uniform kernel function.

3) The human exploration pace gives the second-order information on how fast the human explores the environment. The human may search slower in high potential states and faster in low potential states. The robot should follow the

human's pace. This feature is designed as the probability distribution of the derivative of the state component d_i :

$$H_3\left(\frac{d_i - d_{i-1}}{\tau}\right) = \frac{1}{\Gamma} \sum_{t=2}^{\Gamma} K_U\left(\frac{d_i - d_{i-1}}{\tau}\right) |t \quad (8)$$

where τ is the sample time.

4) The human reaction reveals the third-order information on how the human responds. For example, when the object moves to a dangerous zone or the robot is executing counter-intuitive action, humans may show a fast and strong reaction that causes high acceleration. If the object is safe and the team cooperates well, the human reaction is soft such that the object's acceleration is slow. Thus, the robot also needs to behave like a human. This feature is defined as:

$$H_4\left(\frac{d_i - 2d_{i-1} + d_{i-2}}{\tau^2}\right) = \frac{1}{\Gamma} \sum_{t=3}^{\Gamma} K_U\left(\frac{d_i - 2d_{i-1} + d_{i-2}}{\tau^2}\right) |t \quad (9)$$

Then the reward function is constructed with (6) – (9):

$$V = \alpha P(F|s_t) - \eta + \sum_{m=1}^M \beta_m H_m(s_t) \quad (10)$$

where $H_m(s_t) = \prod_{i=1}^n H_m(d_i)$, which is the joint probability distribution across the state vector. $\alpha \in R$ is a factor in changing the shape of the posterior. β_m are the linear blending weights to scale the features to the same decimal as the posterior and fine-tune each feature's contribution. In this work, the designed weights β_m for each feature are shown in Table 1. $\eta \in R$ is a parameter to control the magnitude of the positive reward region. The robot collects information about the goal specification process during the cooperation (state trajectories). As a result, the reward function evolves to better describe the human's value of the goal, which is specified by both the human and the robot. Thus, we call the updating process EVL (Algorithm 1).

IV. EXPERIMENTS

A. Setup

A ball rolling task was designed (Fig. 2), consisting of a ball on the board. The human and the robot can rotate the board to make the ball roll. The setup accepts multiple players to operate. The ball's movement is the visualizable mark of the HRC formation and goal specification process. The experiment covers dynamic target behavior, indirect control of the target by adjusting the board pose, and the indirect interaction between players, which effectively evaluates the EVL with its interdependent dynamics and uncertainties.

Two environments were designed. Environment 1 (Fig. 3a) evaluates the effectiveness of EVL to learn the dynamics of HRC. It contains a rectangular board with four walls and shifted pivots for both robots. Environment 2 (Fig. 3b) evaluates how the environment's dynamics affect HRC. It uses a square board with two sides of the walls removed. The human and the robot need to find a safe position to prevent the ball from hitting the wall and falling off the board. The human only knows the rough area they feel comfortable in but does not know the exact position because of the unknown dynamics of the environment (i.e., friction, mass, inertia). Fifteen human subjects are invited with the following rules:

1) the human subjects have no prior experience, and 2) the human subjects are not informed with any initial goal position nor the policy of the robot. The human can stop the cooperation if they think the ball stays in a safe position. The experiments were approved by the Institutional Review Board (IRB) of Colorado School of Mines. Prior to participating in the study, a short introduction was provided to the participants including technologies involved, the system setup, and the purpose of the study.

For the RL agent, the state is defined as $s = (x, y)$, which is the 2-D coordinates of the ball related to the board. Based on (4), the human goal's prior probability is following a 2-D Gaussian distribution. The experience is the trajectory of the ball. For both the human and the robot, the actions are roll (x axis) and pitch (y axis) of the board. We developed and compared the performance of two agents that are trained with the SMBI model, one (denoted as EVL) with and the other (denoted as Bayes) without consideration of the human guidance feature, respectively. A baseline model is developed with a pretrained policy that keeps the ball in the initial position, which is the midpoint of the two pivots. The policy does not update during the training (denoted as Fixed).

The environment is first implemented in CoppeliaSim [29], a virtual robot platform with an integrated physics simulation. Two robots are used. One of the robots is controlled by the human, and the RL agent controls the other. After the simulation validation, EVL was tested in a real-world environment with one Kinova MICO arm. One human subject directly holds the other side of the board. The ball position is captured with a webcam at 30Hz using a pattern matching method [30] to achieve real-time processing.

B. Evaluation Metrics

To evaluate EVL in the goal specification process and team performance, the following metrics are defined. The first metric (μ_x, μ_y) and the second metric U are defined to evaluate the goal specification process. The rest are defined for validation which include task performance (L, δ) and cooperation performance (σ, ϕ) after the training. The evaluation metrics are specifically designed to evaluate the HRC on task

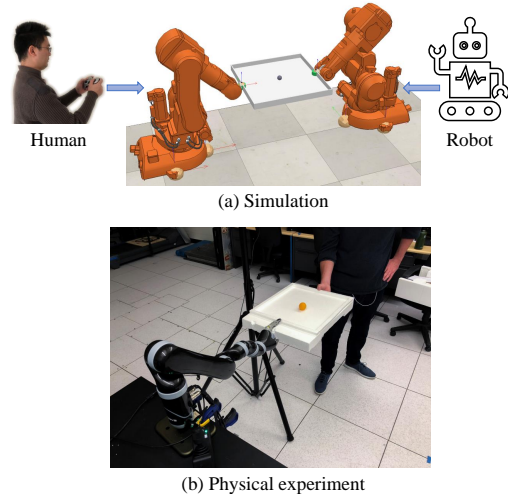


Fig. 2. A ball rolling task in simulation (a) and real-world (b).

and cooperation performance perspectives. Such perspectives can be extended to other tasks with modifications based on specific objectives and experiment setup.

1) The ball trajectory's mean position for each training iteration gives an implicit prediction of the goal position. The mean position (μ_x, μ_y) is calculated as:

$$(\mu_x, \mu_y) = \left(\frac{1}{\Gamma} \sum_{t=1}^{\Gamma} x_t, \frac{1}{\Gamma} \sum_{t=1}^{\Gamma} y_t \right) \quad (11)$$

2) The goal specificity (U) for each training iteration, which is the cumulative divergence (or variance) between the trajectory and the goal position (smaller is better), showing the goal changes from general to specific in training.

$$U = \sum_{t=1}^{\Gamma} \sqrt{(x_t - \mu_x)^2 + (y_t - \mu_y)^2} \quad (12)$$

3) The total ball trajectory length (L) (smaller is better).

$$L = \sum_{t=2}^{\Gamma} \sqrt{(x_t - x_{t-1})^2 + (y_t - y_{t-1})^2} \quad (13)$$

4) The ball's density ratio (δ) is within 5% range around the goal position (larger is better).

$$\delta = \frac{\sum f_r(x, y)}{\Gamma}, 0 \leq \delta < 1 \quad (14)$$

where $f_r(x, y) = \begin{cases} 1, & \text{if } \rho < 0.05\rho_{max} \\ 0, & \text{if } \rho \geq 0.05\rho_{max} \end{cases}$, and $\rho = \sqrt{(x - \mu_x)^2 + (y - \mu_y)^2}$ is the distance between the position (x, y) and the mean (μ_x, μ_y) , and ρ_{max} is the maximum distance.

5) The cumulative effort (σ) (magnitude of actions) that the human executed (smaller is better).

$$\sigma = \sum |a_h| \quad (15)$$

where a_h is the human's action command (i.e., rotation angle), which can be directly accessed and quantified in the simulation environment from the controller's analog input. Note that for the experimental viewpoint, the human effort measures how much physical input the human provides to the task, not the human's mental effort when completing the task.

6) The ratio of agreement (ϕ) in the actions (larger is better).

$$\phi = \frac{\sum ag}{\text{number of actions}}, 0 \leq \phi < 1 \quad (16)$$

where $ag = \begin{cases} 1, & \text{if } a_h \times a_r > 0 \\ 0, & \text{if } a_h \times a_r \leq 0 \end{cases}$, and ag means agreement.

The definition of ag is inspired by Maxwell's Demon Algorithm (MDA) [31]. When human action and robot action are in the same direction, $ag = 1$, otherwise, $ag = 0$.

V. RESULTS

A. Enhanced Goal Specification Process (Training)

The hyper-parameters (shown in Table I) of the EVL and PPO agent are shared across the two tasks for there is no change in the system dynamics except the task objectives. The clip factor improves training stability by limiting the size of the policy change at each step with a clipped surrogate objective function. When computing the discounted sum

of temporal difference errors, the Generalized Advantage Estimator (GAE) is a smoothing factor. The discount factor, learning rate, and the epoch number are the same in simulation and physical experiment, which follow the default setup of the PPO algorithm. The sample time in the physical environment is twice that of the simulation to take into account the action execution time of the physical robot. The episode steps for simulation and physical experiment are correspondingly adjusted to set the episode length to 40 seconds, which is empirically determined in the tuning process through trial and error. A longer episode length may cause distractions to the human subject. A shorter episode length may cause low learning efficiency. The weights α , β_m are designed to amplify each reward component to the same decimal magnitude so that one reward component will not dominant the others. η controls the positive reward region for easier visualization of the reward function and modification of the goal area. Fig. 3 shows the enhanced goal specification processes (training) in simulation and physical experiment. The training results from simulation and physical experiments are consistent in terms of the performance rank for the three methods. Compared to simulation, physical experiments took more time to converge due to the complexity and uncertainty of the physical environment.

The simulation data are cleaner than the physical experiments, therefore were chosen for quantitative analysis. The goal position trace of the ball trajectory shows an example in which the human's behavior is different from the robot's expected optimal goal position. The mean position (μ_x, μ_y) during the goal specification processes for each training iteration are shown in Fig. 4. In environment 1, the human wants to move the ball away from the initial position along the Y -axis. The robot only needs to update its policy related to the Y -axis and keep the X -axis's partial policy. In environment 2, the human tries to find a safe position in the lower-left corner of the board to avoid the ball falling off and hitting the wall. The robot needs to update the policy in both the X -axis and the Y -axis. Ideally, the robot is expected to smoothly contribute to the human's goal specification process with stable policy updating, which relies on an accurate inference of the human's goal. During

TABLE I

HYPER-PARAMETERS OF EVL AND PPO AGENT

Parameters	Simulation	Physical
Experience Horizon	512	256
Entropy Loss Weight	0.02	0.04
Sample Time	0.05	0.1
Episode Step	800	400
Mini-batch Size	64	128
Discount Factor		0.995
Clip Factor		0.05
Learning Rate		0.001
Number of Epoch		3
Weight α		10000
Weight β_1 for H_1		1000
Weight β_2 for H_2		10000
Weight β_3 for H_3		10000
Weight β_4 for H_4		10000
η		10

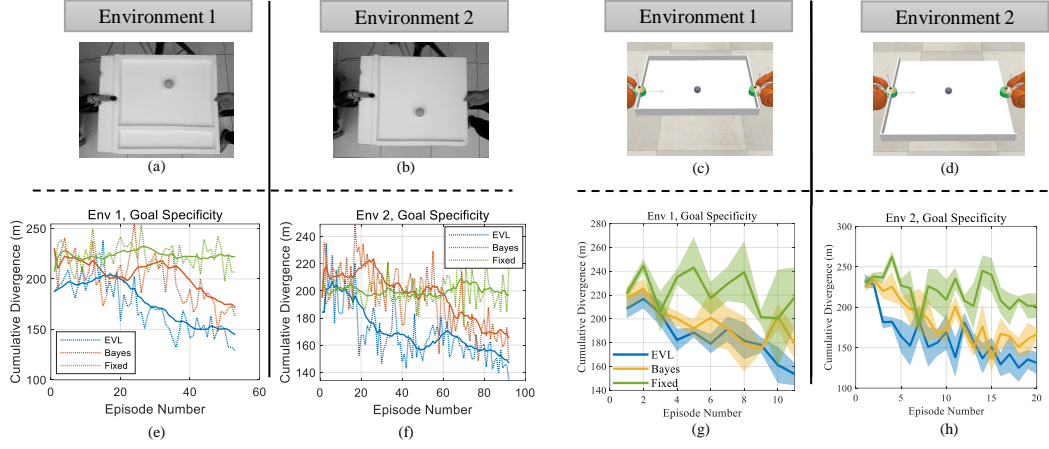


Fig. 3. Enhanced goal specification processes with EVL in simulation and physical experiment. (a)-(d) Environment setups. (e)-(h) The change in mean and variance of the goal specificity during the goal specification process.

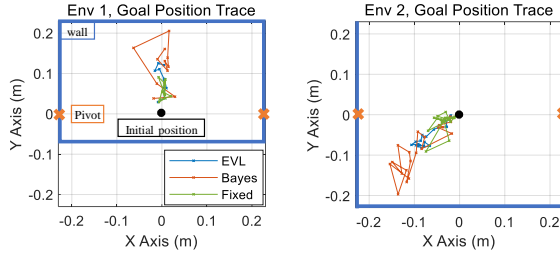


Fig. 4. The goal position trace of the ball trajectory for each iteration of the learning process in simulation.

the early stage of training, the human may show behaviors of varying goal selection when exploring. Such behavior is counter-intuitive from the robot's perspective because it is different from the robot's optimal solution. For example, let us consider environment 2 as shown in Fig. 4, the human tends to roll the ball closer to the wall because it is perceived by the human to be the safer option. However, it is against the robot's initial policy (keep the ball at the center of the board). The robot needs to update its policy to help the human find the goal position. The Bayes method updates based on the online observations of human behaviors, which results in different inferred goals or low inference confidence. This leads to significant changes in robot behavior and reduces both the task and cooperation performance. The fixed policy cannot help the human to specify the goal. It firmly tries to keep the ball at the center of the board. Thus, the goal position trace shows more oscillatory behaviors.

In the simulation, the goal specificity (cumulative divergence), U , at each training iteration is shown in Fig. 3g-3h. A two-sample t-test [32] is applied to determine the significance level of how EVL outperforms baseline methods across the whole training process. Specifically, the p -value is calculated, which is defined as the probability that EVL outperforms the comparison during the training. In this work we look at the single tail comparison to determine if EVL outperforms the other approaches in terms of U . For all tasks, $p < 0.05$ is considered for significance reporting. For environment 1, EVL outperforms Bayes with a $p = 0.0784$ and EVL outperforms Fixed with a $p = 0.0001$. For environment

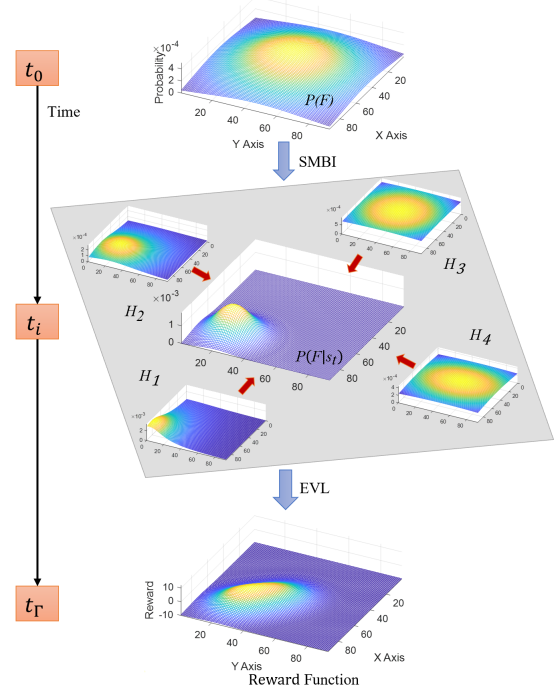


Fig. 5. Visualization of the EVL updating process for environment 2, which starts from t_0 and ends at t_f . The figures in the middle are snapshots of the probability distribution of goal specificity related feature masks at t_i .

2, EVL outperforms the Bayes with a $p = 0.0099$, and EVL outperforms Fixed with a $p = 0.0001$. Therefore, EVL has statistical significance with both approaches for environment 2 and slight lower significance with Bayes for environment 1 when it comes to goal specification. This implies EVL can significantly outperforms Bayes for more difficult tasks. In both environments, the faster goal specification processes of EVL confirm that when humans only have a general goal, the robot needs to utilize the information in the historical observation to assess human behaviors comprehensively. The Bayes method performs worse but still could manage to narrow down the goal specificity in both environments. While the human subject was still familiar with the environment and the partner, the Bayes method mistook the latest observation as the human goal. When the human subject tried to move to the specified goal, it cannot follow and causes a performance

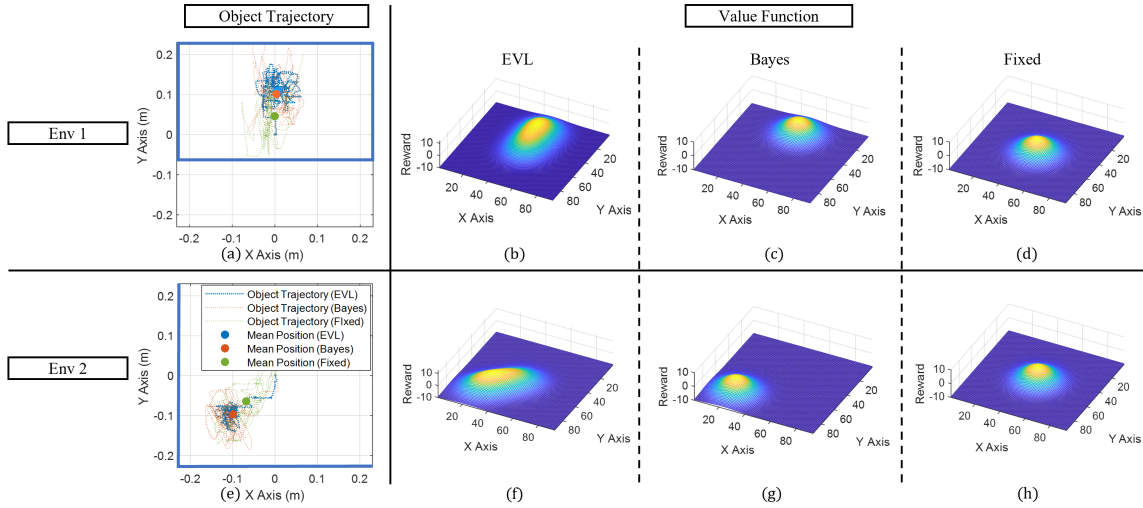


Fig. 6. The object (ball) trajectories and visualizations of the reward functions after the goal clarification process. The top row is for environment 1, and the bottom row is for environment 2.

drop. Thus, it has more performance oscillation throughout the learning process. The RL method with a fixed policy performs worst because no matter how the human acts, the robot always wants to follow its policy (keep the ball at the initial position).

Fig. 5 shows an example of the reward function's updating process for environment 2. The robot has an initial policy. The cooperation starts at the time t_0 . As the cooperation continues at each sample time t_i , the robot utilizes the SMBI method and the goal specificity-related feature masks to generate new reward functions and update its policy. The linear blending weights for each feature mask are tuned to build an appropriate reward function. The final reward function represents the specified human goal is learned at time t_T . The features are designed from literature, which can be expandable and flexible to extract helpful information from the states and their derivatives. Fig. 5 gives insight into why EVL performs better than the baseline methods. The posterior $P(F|s_t)$ that learned from the SMBI method has a distinctive contour compared to the prior $P(F)$. If the agent learns from the updated posterior, the agent cannot update the policy quickly enough to follow the reward function. The robot may spend more time searching for a valid gradient to the goal position. On the contrary, the evolutionary reward function built with EVL connects the contour of the prior $P(F)$ with the posterior $P(F|s_t)$. It provides a smooth and continuous value gradient for the agent to move to the goal position quickly.

B. Enhanced Team Performance (Validation)

Fig. 6 shows the validation of the team performance after the goal specification process. The human and robot cooperate for 40 seconds. During this cooperation process, the robot policy does not update. Fig. 6a-6d are the results for environment 1, including the ball trajectories for the three methods and the corresponding visualized reward functions. Fig. 6e-6h are the results for environment 2. The three methods' different goal positions show that different cooperation processes lead to different goals and team performance.

TABLE II
PERFORMANCE STATISTICS

Env		Task Performance		Cooperation Performance	
		$L(m)$	δ	σ	ϕ
1	EVL	3.44 ± 0.34	0.23 ± 0.06	48.66 ± 3.21	0.68 ± 0.12
	Bayes	4.84 ± 0.42	0.16 ± 0.09	57.59 ± 4.56	0.63 ± 0.19
	Fixed	3.82 ± 0.67	0.18 ± 0.07	53.79 ± 6.28	0.45 ± 0.13
2	EVL	2.14 ± 0.26	0.40 ± 0.07	34.75 ± 4.69	0.64 ± 0.17
	Bayes	5.15 ± 0.37	0.14 ± 0.05	50.82 ± 7.15	0.59 ± 0.22
	Fixed	4.78 ± 0.72	0.11 ± 0.06	47.04 ± 6.84	0.40 ± 0.16

Specifically, the goal positions of EVL and Bayes are away from the initial position, which indicates that the robot has adapted to the human during the cooperation. The Fixed policy's goal positions are closer to the initial position, in which the human had to accommodate more to the robot because the robot cannot adapt. In both environments, the ball trajectories of EVL are tightly distributed around the goal position. The ball trajectories of the baseline methods are more sparsely distributed around the goal position. The reciprocating behavior means there exist more disagreements caused by insufficient assistance.

Table II shows performance statistics to compare team performance under three cooperation methods. Overall, EVL performed better in environment 2 than environment 1, but took a longer time to specify the goal. On average for the two environments, the cooperation achieved with EVL has the shortest trajectory ($L = 2.79m$) and the highest density ratio ($\delta = 0.305$). The human working with the EVL agent spent the least effort ($\sigma = 41.71$). EVL also achieved the highest agreement ratio ($\phi = 0.66$). The longer trajectories and higher human effort of the Bayes method are because the human struggles with the robot's insufficient assistance and spends more effort to correct them; it still helped the human to specify the goal and reduce the disagreement ratio and the human effort compared with the Fixed method. Due to the Fixed policy, the human had to adapt to the robot or even release control. This is why it had shorter trajectories and lower human effort than the Bayes method. However, its disagreement in action and human effort are the highest.

ACKNOWLEDGMENT

This material is based on work supported by the US NSF under grant 1652454 and 2114464. Any opinions, findings, conclusions, or recommendations expressed in this material are those of the authors and do not necessarily reflect those of the National Science Foundation.

REFERENCES

- [1] J. Krüger, T. K. Lien, and A. Verl, "Cooperation of human and machines in assembly lines," *CIRP annals*, vol. 58, no. 2, pp. 628–646, 2009.
- [2] T. Beyl, P. Nicolai, M. D. Comparetti, J. Raczkowski, E. De Momi, and H. Wörn, "Time-of-flight-assisted Kinect camera-based people detection for intuitive human robot cooperation in the surgical operating room," *International journal of computer assisted radiology and surgery*, vol. 11, no. 7, pp. 1329–1345, 2016.
- [3] A. Poncela, C. Urdiales, E. J. Pérez, and F. Sandoval, "A new efficiency-weighted strategy for continuous human/robot cooperation in navigation," *IEEE Transactions on Systems, Man, and Cybernetics Part A: Systems and Humans*, vol. 39, no. 3, pp. 486–500, 2009.
- [4] A. Bauer, D. Wollherr, and M. Buss, "Human–robot collaboration: a survey," *International Journal of Humanoid Robotics*, vol. 5, no. 01, pp. 47–66, 2008.
- [5] T. Bandyopadhyay, K. S. Won, E. Frazzoli, D. Hsu, W. S. Lee, and D. Rus, "Intention-aware motion planning," in *Algorithmic foundations of robotics X*. Springer, 2013, pp. 475–491.
- [6] H. Chaandar Ravichandar, A. Kumar, and A. Dani, "Bayesian human intention inference through multiple model filtering with gaze-based priors," in *FUSION 2016 - 19th International Conference on Information Fusion, Proceedings*. IEEE, 2016, pp. 2296–2302.
- [7] A. Y. Ng and S. Russell, "Algorithms for inverse reinforcement learning," in *Proc. 17th International Conf. on Machine Learning*. Morgan Kaufmann, 2000, pp. 663–670.
- [8] M. Bowman, S. Li, and X. Zhang, "Intent-Uncertainty-Aware Grasp Planning for Robust Robot Assistance in Telemanipulation," in *2019 International Conference on Robotics and Automation (ICRA)*, 2019, pp. 409–415.
- [9] J. F. Fisac, M. A. Gates, J. B. Hamrick, C. Liu, D. Hadfield-Menell, M. Palaniappan, D. Malik, S. S. Sastry, T. L. Griffiths, and A. D. Dragan, "Pragmatic-Pedagogic Value Alignment," *Springer Proceedings in Advanced Robotics*, vol. 10, pp. 49–57, 2020.
- [10] S. Nikolaidis, A. Kuznetsov, D. Hsu, and S. Srinivasa, "Formalizing human-robot mutual adaptation: A bounded memory model," in *ACM/IEEE International Conference on Human-Robot Interaction*, vol. 2016-April. IEEE, 2016, pp. 75–82.
- [11] S. Li, X. Zhang, and J. D. Webb, "3-D-Gaze-Based Robotic Grasping Through Mimicking Human Visuomotor Function for People with Motion Impairments," *IEEE Transactions on Biomedical Engineering*, vol. 64, no. 12, pp. 2824–2835, 2017.
- [12] S. Nikolaidis, Y. X. Zhu, D. Hsu, and S. Srinivasa, "Human-Robot Mutual Adaptation in Shared Autonomy," in *ACM/IEEE International Conference on Human-Robot Interaction*, vol. Part F127194, jan 2017, pp. 294–302.
- [13] J. T. Abbott, J. B. Hamrick, and T. L. Griffiths, "Approximating Bayesian inference with a sparse distributed memory system," in *Proceedings of the 35th Annual Conference of the Cognitive Science Society*, vol. 35, no. 35, 2013, pp. 1686–1691.
- [14] P. Abbeel and A. Y. Ng, "Apprenticeship learning via inverse reinforcement learning," in *Proceedings, Twenty-First International Conference on Machine Learning, ICML 2004*, 2004, pp. 1–8.
- [15] D. Hadfield-Menell, A. Dragan, P. Abbeel, and S. Russell, "Cooperative inverse reinforcement learning," *Advances in Neural Information Processing Systems*, vol. 29, pp. 3916–3924, 2016.
- [16] D. S. Brown and S. Niekum, "Machine teaching for inverse reinforcement learning: Algorithms and applications," in *33rd AAAI Conference on Artificial Intelligence, AAAI 2019, 31st Innovative Applications of Artificial Intelligence Conference, IAAI 2019 and the 9th AAAI Symposium on Educational Advances in Artificial Intelligence, EAAI 2019*, vol. 33, 2019, pp. 7749–7758.
- [17] A. Likmeta, A. M. Metelli, G. Ramponi, A. Tirinzoni, M. Giuliani, and M. Restelli, "Dealing with multiple experts and non-stationarity in inverse reinforcement learning: an application to real-life problems," *Machine Learning*, vol. 110, no. 9, pp. 2541–2576, 2021.
- [18] A. Holzinger, "Interactive machine learning for health informatics: when do we need the human-in-the-loop?" *Brain Informatics*, vol. 3, no. 2, pp. 119–131, 2016.
- [19] L. Pernel, T. Petrič, and J. Babič, "Human-in-the-loop approach for teaching robot assembly tasks using impedance control interface," in *Proceedings - IEEE International Conference on Robotics and Automation*, vol. 2015-June, no. June. IEEE, 2015, pp. 1497–1502.
- [20] W. B. Knox and P. Stone, "Interactively shaping agents via human reinforcement: The TAMER framework," in *K-CAP'09 - Proceedings of the 5th International Conference on Knowledge Capture*, 2009, pp. 9–16.
- [21] D. J. White, "A survey of applications of markov decision processes," *Journal of the Operational Research Society*, vol. 44, no. 11, pp. 1073–1096, 1993.
- [22] J. Schulman, F. Wolski, P. Dhariwal, A. Radford, and O. Klimov, "Proximal Policy Optimization Algorithms," *arXiv preprint arXiv:1707.06347*, 2017.
- [23] W. Chu and Z. Ghahramani, "Preference learning with Gaussian processes," in *ICML 2005 - Proceedings of the 22nd International Conference on Machine Learning*, 2005, pp. 137–144.
- [24] M. Tucker, E. Novoseller, C. Kann, Y. Sui, Y. Yue, J. W. Burdick, and A. D. Ames, "Preference-Based Learning for Exoskeleton Gait Optimization," in *Proceedings - IEEE International Conference on Robotics and Automation*. IEEE, 2020, pp. 2351–2357.
- [25] D. J. C. MacKay, "Bayesian Methods for Backpropagation Networks," in *Models of neural networks III*. Springer, 1996, pp. 211–254.
- [26] J. Xie, Z. Shao, Y. Li, Y. Guan, and J. Tan, "Deep Reinforcement Learning with Optimized Reward Functions for Robotic Trajectory Planning," *IEEE Access*, vol. 7, pp. 105 669–105 679, 2019.
- [27] Y. N. Pan, J. Chen, and X. L. Li, "Spectral entropy: A complementary index for rolling element bearing performance degradation assessment," *Proceedings of the Institution of Mechanical Engineers, Part C: Journal of Mechanical Engineering Science*, vol. 223, no. 5, pp. 1223–1231, 2009.
- [28] B. D. Ziebart, A. Maas, J. A. Bagnell, and A. K. Dey, "Maximum entropy inverse reinforcement learning," in *Proceedings of the National Conference on Artificial Intelligence*, vol. 3. Chicago, IL, USA, 2008, pp. 1433–1438.
- [29] E. Rohmer, S. P. N. Singh, and M. Freese, "V-REP: A versatile and scalable robot simulation framework," in *2013 IEEE/RSJ International Conference on Intelligent Robots and Systems*. IEEE, 2013, pp. 1321–1326.
- [30] N. Zheng, G. Loizou, X. Jiang, X. Lan, and X. Li, "Preface: Computer vision and pattern recognition," *International Journal of Computer Mathematics*, vol. 84, no. 9, pp. 1265–1266, sep 2007.
- [31] A. Broad, I. Abraham, T. Murphey, and B. Argall, "Data-driven Koopman operators for model-based shared control of human-machine systems," *International Journal of Robotics Research*, vol. 39, no. 9, pp. 1178–1195, 2020.
- [32] H. A. David and J. L. Gunnink, "The Paired t Test Under Artificial Pairing," *American Statistician*, vol. 51, no. 1, pp. 9–12, 1997.